Phase-matched second harmonic generation in asymmetric double quantum wells

K. L. Vodopyanov,[a] K. O'Neill, G. B. Serapiglia, and C. C. Phillips
Physics Department, Solid State Group, Imperial College, London SW7 2BZ, United Kingdom

M. Hopkinson
Department of Electrical & Electronic Engineering, University of Sheffield, Sheffield S1 3JD, United Kingdom

I. Vurgaftman and J. R. Meyer
Optical Science Division, Naval Research Laboratory, Washington, DC 20375

(Received 3 December 1997; accepted for publication 23 March 1998)

Efficient ($\sim 1\%$) second harmonic generation, resonantly enhanced near $\lambda = 8.6\ \mu$m, has been observed in asymmetric double multi-quantum well structures. We used (i) edge-emitting waveguide geometry where the phase matching was achieved by incorporating a separate multiple quantum well region which modifies (via the Kramers–Kronig relation) the dispersion of light and (ii) 45° wedge multi-bounce geometry where the phases of second harmonic waves generated at sequential bounces were synchronized by changing the angle of incidence. © *1998 American Institute of Physics.* [S0003-6951(98)03321-X]

As shown recently,[1–3] quantum well structures can be tailored to have giant second and third order intersubband optical nonlinearities, which may be useful for optical frequency conversion, phase conjugation, optical bistability, etc.[4] Greatly enhanced nonlinearities in semiconductor multi-quantum wells (MQWs) look very attractive for efficient generation of new frequencies via frequency mixing and second harmonic generation (SHG). Nonetheless, SHG and difference frequency conversion efficiencies reported so far are rather small ($\ll 1\%$).[5–8] To improve on this, longer interaction lengths are needed, requiring that the phase velocities of the fundamental and second harmonic beams are matched in order to maximize the energy transfer between them.

We report here on the efficient SHG of mid-infrared light, where two different schemes were used to ''phase-match'' the fundamental and second harmonic beams, i.e., to compensate for the natural dispersion of the waveguide material which otherwise leads to dephasing within $\sim 40\ \mu$m.

The structure studied, which is shown schematically in Fig. 1(a), was grown by molecular beam epitaxy and consists of an active SHG region placed between two phase-matching (PM) regions. The active region incorporates 178 periods of repeated asymmetric InGaAs/InAlAs double quantum wells (27 Å $In_{0.53}Ga_{0.47}As$ well–18 Å $In_{0.52}Al_{0.48}As$ barrier–49 Å $In_{0.53}Ga_{0.47}As$ well–100 Å $In_{0.52}Al_{0.48}As$ barrier) with subband resonances close but detuned somewhat from the $\lambda = 8-9\ \mu$m pump wavelength and its second harmonic. The PM region consists of 139 periods of multiple QW (58 Å $In_{0.53}Ga_{0.47}As$ well–100 Å $In_{0.52}Al_{0.48}As$ barrier). Thus, the net epilayer thickness (PM+active layer) was $\approx 8\ \mu$m. The wider (49 Å InGaAs) wells of the active region and the InGaAs wells in the PM region were *n* doped with Si to a sheet carrier concentration 6.5×10^{11} cm^{-2}. The frequencies of the intersubband transitions in the phase-matching QWs were chosen midway between the fundamental and SHG frequencies.[9] The additional dispersion they produce (calculated from the Kramers–Kronig transform of the intersubband absorption line) compensates the normal material dispersion,[10] yet they contribute minimal additional absorption of either beam. Detailed simulations predict that this approach can be used to maintain phase-matching over a long propagation path, much larger than the coherence length.[9]

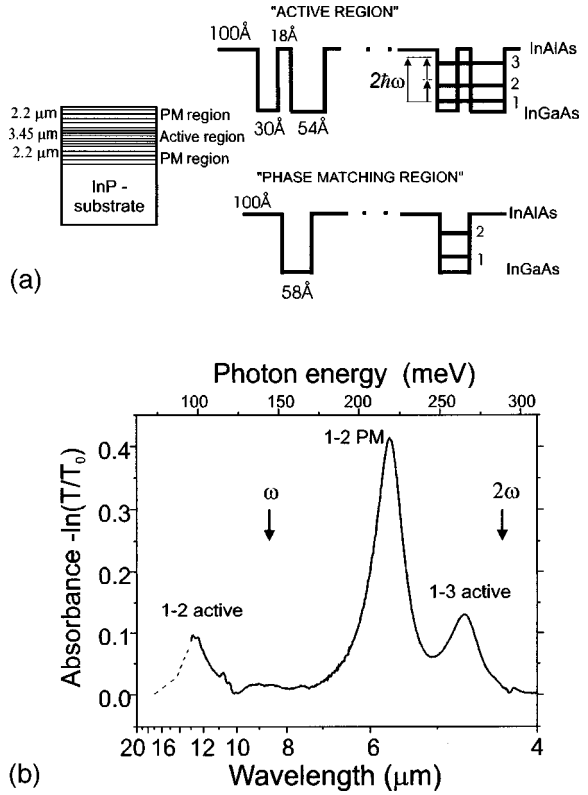

FIG. 1. (a) Design of the ADQW sample for the SHG. (b) Intersubband absorption peaks, corresponding to ''active'' and phase-matching regions.

[a]Electronic mail: k.vodopyanov@ic.ac.uk

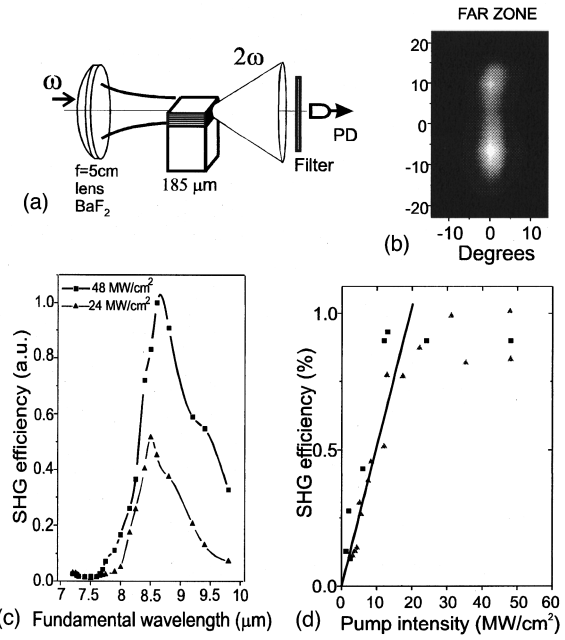

FIG. 2. (a) Schematic of SHG using waveguide mode geometry; (b) Far zone SH beam profile; (c) SHG resonance curves; (d) SHG conversion efficiency ($L=185\ \mu$m) as a function of input intensity.

As a pump source we used a novel traveling-wave optical parametric generator (OPG) based on a nonlinear $ZnGeP_2$ crystal,[11] which was tunable within the range $\lambda=4-10\ \mu$m. The OPG was pumped by single 100 ps pulses ($\lambda=2.8\ \mu$m) from an actively mode-locked, Q-switched and cavity-dumped Cr:Er:YSGG laser–amplifier system (repetition rate 3 Hz). Single OPG pulses with energies of a few μJ and 90 ± 15 ps pulse duration were focused onto the samples (Gaussian profile, $\sim100\ \mu$m beam size) with peak radiation intensity up to 10^8 W/cm^2. Spectral linewidths were typically $10-20$ cm^{-1}, depending on output wavelength.

A linear FTIR absorption spectrum of the ADQW sample [Fig. 1(b)], taken at the Brewster angle (72°) and normalized to that of similar sample with undoped QWs, shows three intersubband absorption peaks—due to the 1–2 and 1–3 transitions in the active layer and the 1–2 transition in the PM layer—with typical widths of 15–20 meV.

Two particular sample geometries were used: (i) ''true'' waveguide [Fig. 2(a)], where the sample was cleaved to make three different lengths L (along the beam propagation) of 105, 185 and 440 μm, and where polarized infrared (IR) pump radiation was coupled onto the edge of the wafer with the electric field vector parallel to the growth direction and (ii) a 45° waveguide geometry [Fig. 4(a)], where the edges were polished at 45° to the growth direction at each end, and the p-polarized light passed into the sample normal to these edges but at 45° to the epitaxial layers. At normal incidence to the polished edge the light reflected five times internally at the epitaxial MQW layer before leaving the sample. In the former geometry, the phase-matching condition was achieved via ''band structure engineering'' of the PM region to modify the dispersion,[9] while in the latter case it was achieved by adjusting the free path length within the InP substrate to make the second harmonics (SH) from consecutive bounces interfere constructively. (Although the PM region was still present in the SHG MQW structure, it did not play a significant role in this case because the path length was short).

A calibrated InSb (77 K) photodiode with a 5.6 μm cutoff was employed for SH detection. The SH signal versus pump wavelength ($L=185\ \mu$m sample) is shown in Fig. 2(b) for two different pump intensities. Small variations of the pump intensity, due to linear absorption by the $ZnGeP_2$ crystal between 8 and 10 μm, were taken into account by normalizing the signal to the input power. The maximum SHG conversion efficiency is peaked at a fundamental wavelength of 8.6 μm—very close to the designed peak value of 8.5 μm.

The far zone SH distribution, obtained by XY scanning in the plane perpendicular to the beam, is shown in Fig. 2(c). The large divergence in the vertical direction is a definite indication of the confinement of the light to the waveguide core and corresponds to the diffraction limit $\sim\lambda/d$, where λ is the SH wavelength (4.3 μm) and d is the waveguide thickness (8 μm). The non-uniformity in this profile is thought to be caused by poor optical quality in the cleaved facet.

The SHG conversion efficiency for the same sample (defined as the ratio of the SH pulse energy to the incoming pump beam energy within the aperture of the waveguide) against pump intensity dependence is shown in Fig. 2(d). We used both attenuating filters and the ''z-scan'' method to vary the intensity of the pump. It is evident that the SHG efficiency is linearly dependent on the pump intensity below 15 MW/cm^2 and remains constant at $\sim0.9\%$ for intensities above that value. While theoretical simulations of the MQW structure predict the loss of phase coherence and reduction in the SHG efficiency at high pump intensities, this effect is blurred under real experimental conditions by the Gaussian spatial and temporal profile of the pump pulses. The maximum theoretical conversion efficiency of $\approx1.5\%$ is in good agreement with the experimental results. The maximum SHG peak power generated at 4.3 μm is 5 W.

Figure 3 compares SHG conversion efficiencies, $\eta_{2\omega}$, for different sample lengths. At $L<200\ \mu$m there is a superlinear increase of $\eta_{2\omega}$ with L, which is a strong argument in favor of the phase-matched interaction. Near 200 μm the conversion efficiency reaches its maximum (it is quite remarkable that our samples were designed to have maximum $\eta_{2\omega}$ near 200 μm) and there is a relatively strong decrease of $\eta_{2\omega}$ at larger length (440 μm), in full accord with the calculations.[9] This is primarily because intensity variations along the beam become too large and it is difficult to maintain coherence along the whole path.

Our analysis of experimental data shows that $\chi^{(2)}$ in our ADQW structure is $\sim50\chi^{(2)}$ of bulk GaAs (the confinement factor of about 0.65 was included). While the highest $\chi^{(2)}$ values reported in the literature for intersubband SHG are $\sim1900\chi^{(2)}_{GaAs}$,[3] those works assumed double resonance. We intentionally detuned the structure in order to get [Fig. 1(b)] much lower linear absorption (a few % of that of the peak).

In the 45° waveguide geometry, the SH is generated only while the light passes through the MQW epilayer (we neglect bulk SHG in the InP substrate). To get maximum conversion efficiency the SH generated at each reflection must interfere constructively with the SH generated at previ-

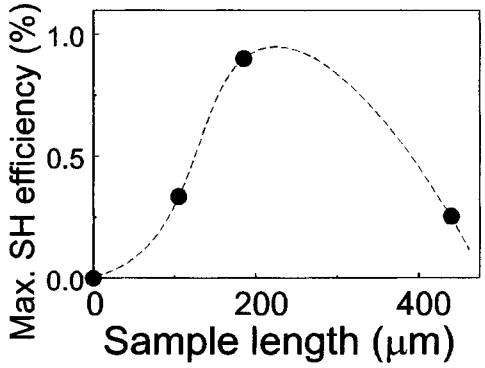

FIG. 3. SHG conversion efficiency vs sample length. Pump intensity ~ 50 MW/cm^2. Dashed curve—a trace for an eye.

ous reflections within the structure. Using a generalized phase-matching condition, i.e.,

$$2k_\omega L = k_{2\omega} L + 2m\pi, \tag{1}$$

where $k_{2\omega}$ and k_ω are the magnitudes of the wave vectors of the SH and fundamental beams, respectively, $L = L_1 + L_2$ is the distance traveled by the light beam in the substrate between reflections at the epitaxial layer [Fig. 4(a)], and m is an integer. The main idea of the phase matching here is that by tilting the sample we can change $L_1 + L_2$ and thus maximize the SH output. In fact, the angular tuning curve in Fig. 4(b) shows PM periodic resonances spaced by 29.9°. This agrees perfectly with the calculated value of 30°, where we assumed an average sample thickness of 243 μm, InP refractive index[12] $n_\omega = 3.1$, and $(n_{2\omega} - n_\omega) = 3.7 \times 10^{-2}$.

The width of the peaks ($\delta\varphi \approx 5.5°$) is close to what one would expect from a simple interferometer ''finesse'' consideration: the ratio of the separation between the fringes to their width is of the order of the number of interfering beams (5 in our case). However $\delta\varphi$ may also be affected by the finite beam divergence.

Figure 4(c) compares the far zone distributions of light intensity for the pump and SH beams for the 45° wedge geometry. The SH beam is cylindrically symmetric and has a divergence of approximately half that of the pump [5° full width half maximum (FWHM) as compared to 10°]. This is related to the smaller diffraction effect for the SH, which has half as long a wavelength and approximately the same beam size.

The SHG conversion efficiency [Fig. 4(d)] in a 45° waveguide was found to increase linearly with pump intensity, and did not saturate up to a maximum intensity of 100 MW/cm^2. A maximum $\eta_{2\omega} = 0.2\%$ was measured. The absence of saturation and lower SHG efficiency (compared to the true waveguide) may be explained by weaker coupling to intersubband transitions in this geometry, i.e., the pump E vector is not parallel to the growth axis. The maximum peak SHG power was over 30 W in this geometry, which is, despite the lower efficiency, larger than that for the true waveguide and is the result of better coupling of the pump into the waveguide. As expected, the measured SH polarization in both geometries was the same as that of the pump (i.e., vertical in Figs. 2 and 4) corresponding to the only nonzero nonlinear-optical tensor component d_{33}.

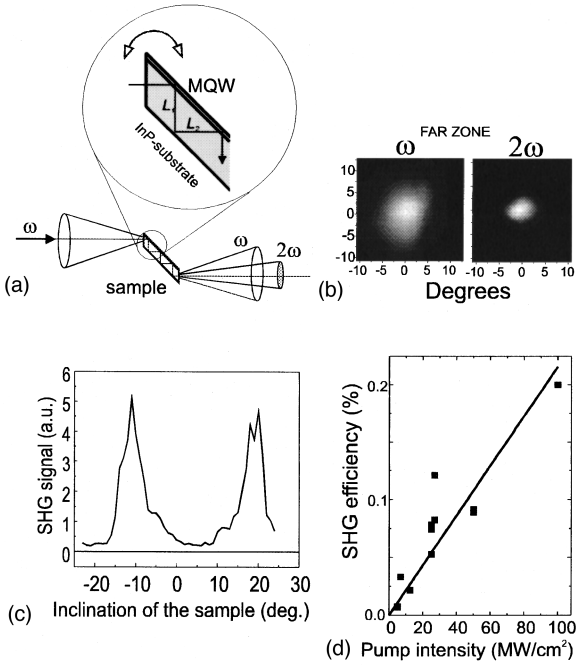

FIG. 4. (a) Schematic of SHG using 45° wedge geometry with five double passes; (b) Far zone profiles of the fundamental and SH beams; (c) SH intensity plotted against the angle of the sample; (d) SHG conversion efficiency as a function of input intensity.

In conclusion, we have demonstrated phase-matched intersubband-based SHG in quantum well waveguides with relatively long interaction lengths. Resonant enhancement near the fundamental $\lambda = 8.6$ μm was obtained, very close to the designed $\lambda = 8.5$ μm, with a maximum conversion efficiency of 0.2% for the 45° wedge geometry and 0.9% (at 15 MW/cm^2) for the true waveguide geometry. This value for SHG conversion efficiency is, to our knowledge, the highest ever obtained for intersubband-based nonlinearities.

The authors would like to thank Geoff Hill from the Department of Electrical & Electronic Engineering, University of Sheffield for the sample processing. This work has been supported by the UK Engineering and Physical Sciences Research Council.

[1] M. M. Fejer, S. J. B. Yoo, R. L. Byer, A. Harwit, and J. S. Harris, Jr., Phys. Rev. Lett. **62**, 1041 (1989).
[2] E. Rosencher, P. Bols, J. Nagle, and S. Delaitre, Electron. Lett. **25**, 1063 (1989).
[3] P. Boucaud, F. H. Julien, D. D. Yang, and J.-M. Lourtioz, Appl. Phys. Lett. **57**, 215 (1990).
[4] G. Almogy and A. Yariv, J. Nonlinear Opt. Phys. Mater. **4**, 401 (1995).
[5] P. Boucaud, F. H. Julien, D. D. Yang, J.-M. Lourtioz, E. Rosencher, and P. Bois, Opt. Lett. **16**, 199 (1991).
[6] Z. Chen, M. Li, D. Cui, H. Lu, and G. Yang, Appl. Phys. Lett. **62**, 1502 (1993).
[7] C. Sirtori, F. Capasso, J. Faist, L. N. Pfeiffer, and K. W. West, Appl. Phys. Lett. **65**, 445 (1994).
[8] H. C. Chui, G. L. Woods, M. M. Fejer, E. L. Martinet, and J. S. Harris, Jr., Appl. Phys. Lett. **66**, 265 (1995).
[9] I. Vurgaftman, J. R. Meyer, and L. R. Ram-Mohan, IEEE J. Quantum Electron. **32**, 1334 (1996).
[10] G. Almogy and A. Yariv, Opt. Lett. **19**, 1192 (1994).
[11] K. L. Vodopyanov, J. Opt. Soc. Am. B **10**, 1723 (1993); K. L. Vodopyanov and V. Chazapis, Opt. Commun. **135**, 98 (1997).
[12] A. N. Pikhtin and A. D. Yaskov, Sov. Phys. Semicond. **12**, 622 (1978).